PHYSICAL REVIEW FLUIDS 1, 060504 (2016)

Electrohydrodynamic instabilities of viscous drops*

Petia M. Vlahovska
School of Engineering, Brown University, Providence, Rhode Island 02912, USA
(Received 6 July 2016; published 18 October 2016)

A classic result due to Taylor is that a weakly conducting drop bearing zero net charge placed in a uniform electric field adopts a prolate or oblate spheroidal shape, the flow and shape being axisymmetrically aligned with the applied field. Here I overview some intriguing symmetry-breaking instabilities occurring in strong applied dc fields: Quincke rotation resulting in drop steady tilt or tumbling, and pattern formation on the surface of a particle-coated drop.

DOI: 10.1103/PhysRevFluids.1.060504

I. INTRODUCTION

Electric fields provide a versatile means to generate and manipulate small-scale fluid and particle motion. Weakly conducting fluids (leaky dielectrics) allow free charge to accumulate at interfaces where the tangential electric stresses, due to the electric field acting on the induced charge, drag fluids into motion [1].

The dynamics and stability of fluid-fluid interfaces, stressed by an applied electric field, have been extensively studied since the pioneering works of Taylor [2–4]. Interest in electrohydrodynamic instabilities has been fueled by many intriguing observations. For example, thin polymer films form periodic arrays of pillars when subjected to a vertical dc [5,6] or ac electric field [7,8]. Drops, bearing no net charge, can form conical tips at poles and emit jets of charged microdroplets [9–11], a phenomenon common to a wide range of applications such as printing, electrospinning, and electrosprays. More recently, suspensions of colloidal particles subjected to external electric fields were found to self-organize into large-scale structures [12–14] such as bands [15,16] or undergo spontaneous directed motion [17,18]. Confinement, as in the case of particles trapped on fluid interfaces, plays an important but largely unexplored role in the instabilities and pattern formation [19,20].

Here I overview some recent intriguing research on drop dynamics and instabilities in an applied uniform dc electric field. Even though I will attempt to acknowledge all relevant contributions to this topic of resurgent interest, the selection may be far from exhaustive as I will mainly focus on work from my group.

II. QUINCKE ROTATION OF A DROPLET

A. Quincke effect

The spontaneous spinning of a rigid sphere in a uniform dc electric field has been known for over a century [1,21,22], although this phenomenon has been largely overlooked until the recent interest in "active" suspensions (collections of motile colloids, in particular, Quincke rollers) [17,23–25].

The phenomenon arises from particle polarization in an applied electric field due to the accumulation of free charges at the particle interface [1]. The induced dipole due to these free charges lags behind the application of the uniform dc electric field

$$\mathbf{P} = (\chi_0 - \chi_\infty)\mathbf{E}[1 - \exp(-t/t_{\mathrm{MW}})], \tag{1}$$

*This paper is based on an invited lecture given by Petia M. Vlahovska at the 68th Annual Meeting of the APS Division of Fluid Dynamics, which was held 22–24 November 2015 in Boston (MA), USA.

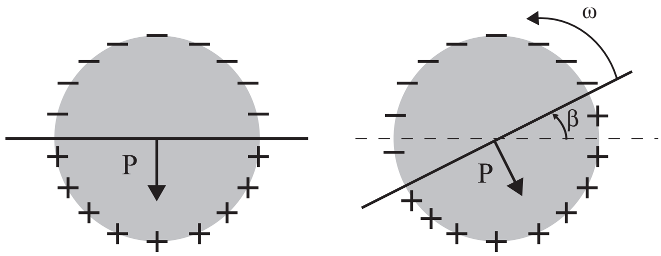

FIG. 1. Charge distribution in unstable equilibrium for a sphere with $R/S < 1$. Above a critical field strength $E_0 > E_Q$, where $E_0 = |\mathbf{E}|$ and E_Q is given by Eq. (8), constant rotation around an axis perpendicular to the electric field is induced by the misaligned dipole moment of the particle (right). The rotation can be either clockwise or counterclockwise [21,26,27].

where χ_0 and χ_∞ are the low- and high-frequency susceptibilities of the particle. For a sphere with radius a,

$$\chi_0 - \chi_\infty = 4\pi\varepsilon_s a^3 \frac{3(R-S)}{(R+2)(S+2)}, \tag{2}$$

where R and S characterize the mismatch of electrical conductivity σ and permittivity ε between the sphere and the suspending fluid

$$R = \frac{\sigma_p}{\sigma_s}, \quad S = \frac{\varepsilon_p}{\varepsilon_s}. \tag{3}$$

The subscripts p and s denote the values for particle and suspending medium, respectively, and the Maxwell-Wagner polarization time t_{MW} is the characteristic time scale for polarization relaxation

$$t_{\mathrm{MW}} = \frac{\varepsilon_p + 2\varepsilon_s}{\sigma_p + 2\sigma_s}. \tag{4}$$

For rotation to occur, the induced dipole moment of the sphere has to be oriented opposite to the direction of the applied field ($R/S < 1$) [see Eqs. (1) and (2)]. This configuration is unfavorable and becomes unstable above a critical strength of the electric field. A perturbation can displace the dipole and the resulting torque induces physical rotation of the sphere (around an axis perpendicular to the applied field direction).

For rotation to be sustained, the rotation period should be comparable to the Maxwell-Wagner polarization time. This condition ensures that while the induced surface-charge distribution rotates with the sphere, the exterior fluid can recharge the interface. The balance between charge convection by rotation and supply by conduction from the bulk results in an oblique dipole orientation shown in Fig. 1.

The rotation rate ω of the Quincke rotor is determined from the conservation of angular momentum of the sphere [26,27]

$$I\frac{d\omega}{dt} = P_\perp E - \alpha\omega, \tag{5}$$

where $I = 8\pi\rho_p a^5/15$ is the moment of inertia and $\alpha = 8\pi\mu_s a^3$ is the friction factor of the sphere. The dipole component orthogonal to the filed direction $P_\perp$ is determined from the equations for the polarization evolution

$$\frac{dP_\perp}{dt} = -\omega P_{||} - t_{\mathrm{MW}}^{-1} P_\perp, \quad \frac{dP_{||}}{dt} = \omega P_\perp - t_{\mathrm{MW}}^{-1}[P_{||} - (\chi_0 - \chi_\infty)E]. \tag{6}$$

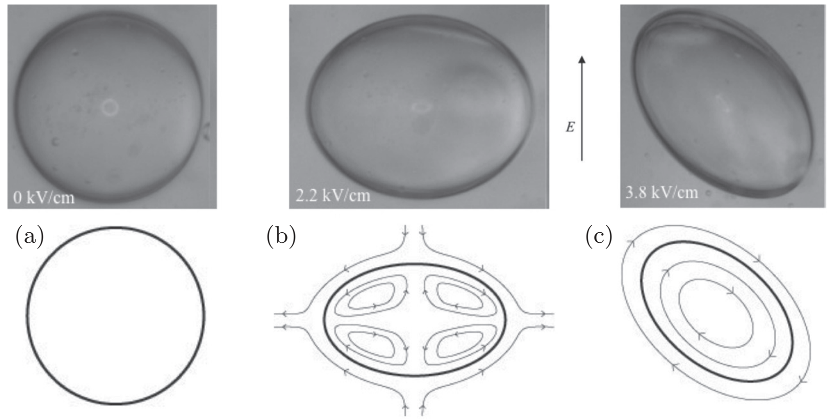

FIG. 2. (a) Sketch illustrating drop shape and flow streamlines in a uniform dc electric field with increasing strength. (b) The drop is spherical in the absence of electric field. (c) Weak fields induce pure straining flow and axisymmetric oblate deformation in the case $R < S$. In strong fields, the flow acquires a rotational component and the drop is tilted with respect to the applied field direction.

Steady-state solutions of Eqs. (5) and (6) are no rotation [with $\omega = 0$, induced dipole $P_{||}$ given by Eq. (1), and $P_\perp = 0$] and steady rotation with

$$\omega = \pm\frac{1}{t_{\rm MW}}\sqrt{\frac{E^2}{E_Q^2} - 1}, \quad P_\perp = \frac{\alpha\omega}{E}, \tag{7}$$

where the $\pm$ sign reflects the two possible directions of rotation and

$$E_Q^2 = \frac{2\sigma_s\mu_s(R+2)^2}{3\varepsilon_s^2(S-R)}. \tag{8}$$

Equation (7) shows that rotation is possible only if the electric field exceeds a critical value given by E_Q; notably, the rotation rate is independent of particle size. A more detailed analysis shows that the transition to rotation occurs via a pitchfork bifurcation [21,27]. Intriguingly, the set of three equations, i.e., evolution of the two dipole components (parallel and perpendicular to the applied field direction) [Eq. (6)] and conservation of angular momentum [Eq. (5)], map onto to the Lorenz equations [28] and show that the second bifurcation occurs at stronger fields resulting in chaotic rotation (random reversals of rotation direction) [21,29].

B. Drop electrorotation

Particle fluidity increases complexity. The electric field acting on the induced surface charge creates normal stresses that deform the drop into an ellipsoid and shear stresses that drag the fluids into motion. In the Taylor regime (nearly spherical drop and no electrorotation), the fluid undergoes axisymmetric straining flow about the drop [4] [see Fig. 2(b)] with surface velocity

$$u_\theta = \frac{a\varepsilon_s E_0^2}{\mu_s}\frac{9(S-R)}{10(1+\lambda)S(R+2)^2}\sin(2\theta), \tag{9}$$

where $\lambda = \mu_p/\mu_s$ is the viscosity ratio and θ is the angle with the field direction. Above a threshold electric field, which is in general different from Eq. (8), the flow acquires a rotational component due to the Quincke effect and experiments show that the deformed droplet can assume a steady tilted orientation relative to the applied field [30–32] [see Fig. 2(c)] or undergo irregular rotational motions [33,34] (see Fig. 3). If drop viscosity is high, the ellipsoidal drop tumbles [see Fig. 3(b)] while randomly reversing the direction of rotation. A low-viscosity drop, however, can undergo additional

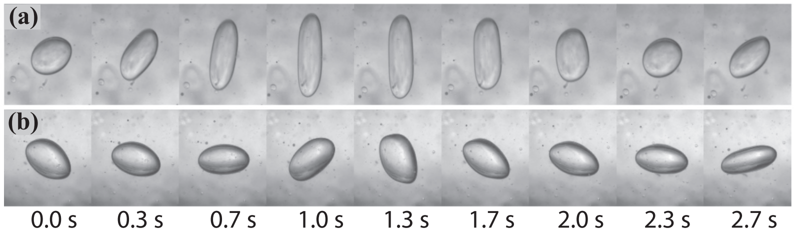

FIG. 3. Examples of unsteady drop behavior in a uniform dc electric field [34]: (a) viscosity ratio $\lambda = 1$, field strength $E_0 = 9.9$ kV/cm, and drop radius $a = 1.8$ mm and (b) $\lambda = 14$, $E_0 = 9.7$ kV/cm, and $a = 3.0$ mm. The experimental system is a silicon oil drop suspended in castor oil, $t_{\mathrm{MW}} = 1.3$ s, and $E_Q = 2.7$ kV/cm.

deformation while rotating [see Fig. 3(a)]. The resulting shape variations resemble oscillations (see Fig. 4).

The steady tilt is well understood [32,35]. Analytical models, which assume small deformations and charge convection dominated by the rotational flow, agree only with the experimental data for high-viscosity drops [32] but do not capture the increased threshold for electrorotation and shape variations with field strength of low-viscosity drops.

The time-dependent tumblinglike dynamics, however, remains to be explained. Anisotropy in the polarization relaxation due to the nonspherical shape can give rise to similar behavior [34]. Indeed, rigid ellipsoids are predicted theoretically to align, swing, or tumble [36,37] (although these behaviors are only recently being probed experimentally [38]). Including shape variations as observed in the case of the low-viscosity drop is analytically challenging and tractable only by fully-three-dimensional numerical simulations. Such simulations are, however, currently unavailable as all three-dimensional computational analyses of drop electrohydrodynamics are restricted to axisymmetric geometries [39–41].

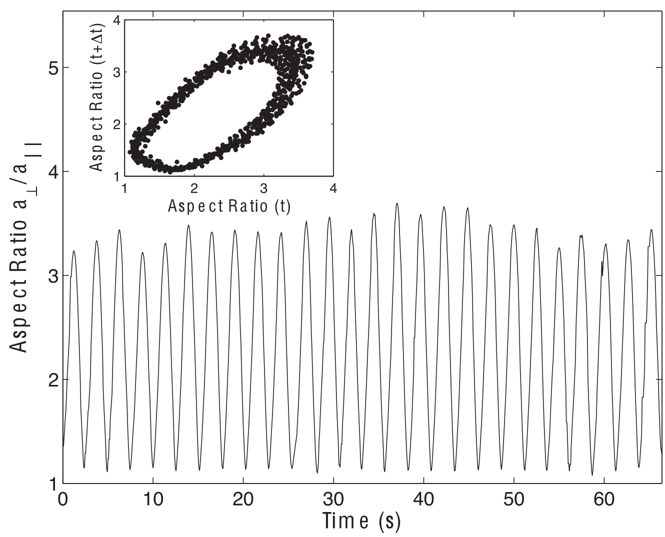

FIG. 4. Evolution of the aspect ratio in real time and in time-delay plots with $\Delta t = t_{\mathrm{MW}}/4$ (inset) for the drop shown in Fig. 3(a).

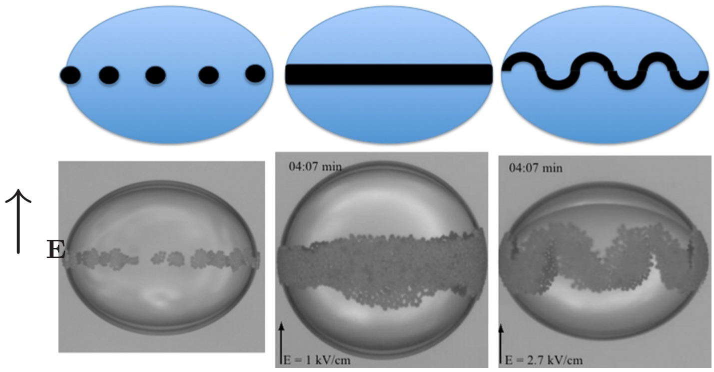

FIG. 5. Polyethylene microspheres (diameter 50 μm), initially randomly distributed at the surface of a silicon oil drop suspended in castor oil, can assemble at the equator into nearly circular patches, a continuous belt, or a sinusoidally shaped ribbon (see [45]).

III. INTERFACIALLY COMPLEX DROP: PARTICLES AND SURFACTANTS

Fluid interfaces allow adsorbed particles and surfactants to move laterally and be convected by flow. In the Taylor regime (9), the surfactants or particles accumulate at either the drop tips or the equator depending on the flow direction. The redistribution of surfactant has different effects on drop electrohydrodynamics than surface-adsorbed particles, even though colloidal particles are often considered to act as surfactants [42].

A. Weak electric fields

Nonuniform surfactant coverage generates Marangoni stresses that at equilibrium immobilize the interface [43,44]. As a result, at steady state there is no flow and the drop shape is independent of the viscosity ratio and surfactant elasticity

$$D = \mathrm{Ca}\frac{9[(1+R)^2 - 4S]}{16(2+R)^2}. \tag{10}$$

Surfactant elasticity β enters implicitly through the definition of the capillary number

$$\mathrm{Ca}_0 = \mathrm{Ca}(1+\beta)^{-1}, \quad \beta = \frac{\gamma_0 - \gamma_{\mathrm{eq}}}{\gamma_{\mathrm{eq}}}. \tag{11}$$

Here $\mathrm{Ca}_0 = \varepsilon_s E^2 a/\gamma_0$ is defined for a clean, surfactant-free drop with interfacial tension γ_0, while Ca is defined based on the equilibrium surface tension of the surfactant-covered interface γ_{eq}. Drop deformation is enhanced compared to clean interfaces.

In contrast, surface adsorbed particles suppress the flow only at high coverage (greater than 90%); at low coverages the flow persists in the clean (free of particles) spots (e.g., the area not covered by the particle belt seen in Fig. 5). Drop deformation cannot be described by Eq. (10); instead a capsule model, which treats the particle monolayer as an elastic sheet, works best [46].

B. Strong electric fields and drop destabilization

Application of strong electric field leads to different instabilities depending on the base Taylor flow direction (9). If $R/S > 1$ the surface flow is from the equator to the pole and tip streaming can occur from cones formed at the opposite poles of the prolate drop [10,44,47,48].

In the case $R/S < 1$ the surface flow is from the pole to the equator and the equator is a stagnation ring. Surfactant accumulation at the equator lowers the surface tension and thus can destabilize the stagnation ring [49]. The oblate drop flattens and forms a sharp rim, from which tiny drops

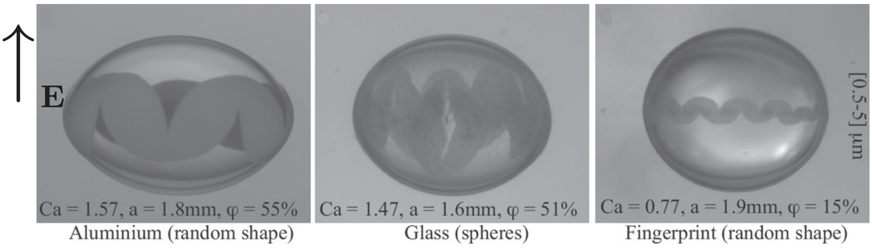

FIG. 6. Microparticles (radius $r = 0.5$–$5\ \mu$m) of different conductivity and shape all form a belt that undergoes buckling instability. The electric stress scaled by surface tension stresses is denoted by Ca, φ is the surface coverage, and a denotes the drop radius.

are emitted (equatorial streaming) [50]. The effects of surfactant on droplet electrohydrodynamics, however, remain largely unexplored.

Surface-adsorbed colloidal particles also accumulate at the equator and form a belt if $R/S < 1$ (see Fig. 5) [19,20,46,51,52]. However, in stronger fields the belt destabilizes: It buckles and forms a variety of surface patterns depending on coverage, such as an undulating belt around the equator or isolated, rotating clusters of particles. The undulating belt itself is a dynamic structure and consists of segments within which particles move in closed orbits.

Experiments have shown that particles move to the equator for a very broad range of particle conductivities [20] (see Fig. 6). Hence, the formation of the equatorial belt is likely driven not by electrostatic interactions (dielectrophoresis or dipole-dipole interactions) but by the flow.

To see this, we can estimate the relative importance of particle dielectrophoresis (which is the dipole translation driven by a gradient in the electric field) and convection by comparing the magnitudes of the electrohydrodynamic and the dielectrophoretic velocities. The first one v_e can be estimated from the solution for the electrohydrodynamic flow around a spherical drop [Eq. (9)],

$$v_e \sim a\varepsilon_s E_0^2 / \mu_s. \tag{12}$$

The dielectrophoretic velocity v_d is obtained by balancing the dielectrophoretic force and hydrodynamic drag

$$v_d \sim \left(\varepsilon_s r^3 K_{\mathrm{CM}} E_0^2 / a\right) / \mu_s r, \tag{13}$$

where r is the particle radius and $K_{\mathrm{CM}} = (\sigma_p - \sigma_s)/(\sigma_p + 2\sigma_s)$ denotes the Clausius-Mossotti factor for a sphere. Comparing these two, we see that indeed dielectrophoresis is much weaker than convection $v_e/v_d \sim a^2/r^2 \gg 1$.

The mechanism responsible for the belt buckling and breakup into patches remains unknown. Specifically, it is not clear if this is a result of (i) a hydrodynamic instability (occurring even in the absence of particles) [49] or (ii) self-organization emerging from the collective particle dynamics [25,53]. There is evidence favoring both explanations. In favor of the instability, (i), Tseng and Prosperetti recently showed [49] that the convergent flow near a zero vorticity point can become unstable and that a local perturbation can grow due to kinematic compression and viscous stresses. In the classical example of tip streaming [47,48], if surfactants are present, they are carried by the flow toward the zero-vorticity point and weaken the action of surface tension, which is the only physical mechanism countering the instability. In our case, however, surfactants are absent and it is unclear how the electric field and possibly charge convection drive this type of instability. Evidence in favor of self-organization, (ii), was presented using a simple model of particles trapped on the drop interface. We have simulated the collective dynamics of a monolayer of spheres driven by constant clockwise or counterclockwise torques [25]. The emergence of patterns, resembling those seen in experiments, such as traffic lanes or large vortices comprised of same-type rotors was observed. A more refined model [53], which includes dipole-dipole and hydrodynamic interactions between the particles, also shows structuring similar to the experiment.

IV. CONCLUSION AND OUTLOOK

Electrohydrodynamics is undergoing a renaissance that has been inspired by the scientific intrigue of the recently discovered instabilities of drops reviewed here, as well as the integration of electrokinetic and electrohydrodynamic theories [54,55], which is bringing these two fields closer. The emergent behavior and intricate patterns formed by surface- trapped particles in electric fields could provide novel ways to create structurally complex materials with tailored optical, mechanical, magnetic, or electric properties. Suspensions of hard (colloidal sphere) and soft (drop) Quincke rotors are a new class of active matter, which is virtually unexplored. Other soft particles with complex interfacial mechanics such as vesicles [56–58] also undergo fascinating electrohydrodynamic instabilities (formation of edges, reversible poration, and phase separation). I hope that the questions defined in this paper will inspire further research in the area of electrohydrodynamics of complex interfaces.

ACKNOWLEDGMENT

This work was supported by NSF-CBET Awards No. 1132614, No. 1437545, and No. 1544196.

[1] J. R. Melcher and G. I. Taylor, Electrohydrodynamics—A review of role of interfacial shear stress, Annu. Rev. Fluid Mech. **1**, 111 (1969).
[2] G. I. Taylor and A. D. McEwan, The stability of a horizontal fluid interface in a vertical electric field, J. Fluid Mech. **22**, 1 (1965).
[3] G. I. Taylor, Disintegration of water drops in an electric field, Proc. R. Soc. London Ser. A **280**, 383 (1964).
[4] G. I. Taylor, Studies in electrohydrodynamics. I. Circulation produced in a drop by an electric field, Proc. R. Soc. London Ser. A **291**, 159 (1966).
[5] E. Schaffer, T. Thurn-Albrecht, T. P. Russell, and U. Steiner, Electrically induced structure formation and pattern transfer, Nature (London) **403**, 874 (2000).
[6] N. Wu and W. B. Russel, Micro- and nano-patterns created via electrohydrodynamic instabilities, Nanotoday **4**, 180 (2009).
[7] S. A. Roberts and S. Kumar, AC electrohydrodynamic instabilities in thin liquid films, J. Fluid Mech. **631**, 255 (2009).
[8] P. Gambhire and R. M. Thaokar, Electrohydrodynamic instabilities at interfaces subjected to alternating electric field, Phys. Fluids **22**, 064103 (2010).
[9] R. T. Collins, K. Sambath, M. T. Harris, and O. A. Basaran, Universal scaling laws for the disintegration of electrified drops, Proc. Natl. Acad. Sci. USA **110**, 4905 (2013).
[10] R. T. Collins, J. J. Jones, M. T. Harris, and O. A. Basaran, Electrohydrodynamic tip streaming and emission of charged drops from liquid cones, Nat. Phys. **4**, 149 (2008).
[11] J. F. de la Mora, The fluid dynamics of taylor cones, Annu. Rev. Fluid. Mech. **39**, 217 (2007).
[12] A. van Blaaderen, M. Dijkstra, R. van Roij, A. Imhof, M. Kamp, B. W. Kwaadgras, T. Vissers, and B. Liu, Manipulating the self assembly of colloids in electric fields, Eur. Phys. J. Spec. Top. **222**, 2895 (2013).
[13] I. S. Aranson, Collective behavior in out-of-equilibrium colloidal suspensions, C. R. Phys. **14**, 518 (2013).
[14] J. Dobnikar, A. Snezhko, and A. Yethiraj, Emergent colloidal dynamics in electromagnetic fields, Soft Matter **9**, 3693 (2013).
[15] J. P. Singh, P. P. Lele, F. Nettesheim, N. J. Wagner, and E. M. Furst, One- and two-dimensional assembly of colloidal ellipsoids in ac electric fields, Phys. Rev. E **79**, 050401 (2009).
[16] H. R. Vutukuri, S. Badaire, D. A. Matthijs de Winter, A. Imhof, and A. van Blaaderen, Directed self-assembly of micron-sized gold nanoplatelets into oriented flexible stacks with tunable interplate distance, Nano Lett. **15**, 5617 (2015).

[17] A. Bricard, J.-B. Caussin, N. Desreumaux, O. Dauchot, and D. Bartolo, Emergence of macroscopic directed motion in populations of motile colloids, Nature (London) **503**, 95 (2013).
[18] A. Bricard, J.-B. Caussin, D. Das, C. Savoie, V. Chikkadi, K. I. Shitara, O. Chepizhko, F. Peruani, D. Saintillan, and D. Bartolo, Emergent vortices in populations of colloidal rollers, Nature Comm. **6**, 7470 (2015).
[19] P. Dommersnes, Z. Rozynek, A. Mikkelsen, R. Castberg, K. Kjerstad, K. Hersvik, and J. Fossum, Active structuring of colloidal armor on liquid drops, Nat. Commun. **4**, 2066 (2013).
[20] M. Ouriemi and P. M. Vlahovska, Electrohydrodynamics of particle-covered drops, J. Fluid Mech. **751**, 106 (2014).
[21] E. Lemaire and L. Lobry, Chaotic behavior in electro-rotation, Physica A **314**, 663 (2002).
[22] G. Quincke, Ueber rotation em im constanten electrischen felde, Ann. Phys. Chem. **295**, 417 (1896).
[23] A. Snezhko, Complex collective dynamics of active torque-driven colloids at interfaces, Curr. Op. Colloid Interface Sci. **21**, 65 (2016).
[24] O. D. Lavrentovich, Active colloids in liquid crystals, Curr. Op. Colloid Interface Sci. **21**, 97 (2016).
[25] K. Yeo, E. Lushi, and P. M. Vlahovska, Collective Dynamics in a Binary Mixture of Hydrodynamically Coupled Microrotors, Phys. Rev. Lett. **114**, 188301 (2015).
[26] T. B. Jones, Quincke rotation of spheres, IEEE Trans. Ind. Appl. **20**, 845 (1984).
[27] I. Turcu, Electric field induced rotation of spheres, J. Phys. A **20**, 3301 (1987).
[28] S. H. Strogatz, *Nonlinear Dynamics and Chaos: With Applications to Physics, Biology, Chemistry, and Engineering* (Perseus Books, Cambridge, 1994).
[29] F. Peters, L. Lobry, and E. Lemaire, Experimental observation of Lorenz chaos in the Quincke rotor dynamics, Chaos **15**, 013102 (2005).
[30] J. W. Ha and S. M. Yang, Electrohydrodynamics and electrorotation of a drop with fluid less conductive than that of the ambient fluid, Phys. Fluids **12**, 764 (2000).
[31] P. F. Salipante and P. M. Vlahovska, Electrohydrodynamics of drops in strong uniform dc electric fields, Phys. Fluids **22**, 112110 (2010).
[32] H. He, P. F. Salipante, and P. M. Vlahovska, Electrorotation of a viscous droplet in a uniform direct current electric field, Phys. Fluids **25**, 032106 (2013).
[33] H. Sato, N. Kaji, T. Mochizuki, and Y. H. Mori, Behavior of oblately deformed droplets in an immiscible dielectric liquid under a steady and uniform electric field, Phys. Fluids **18**, 127101 (2006).
[34] P. F. Salipante and P. M. Vlahovska, Electrohydrodynamic rotations of a viscous droplet, Phys. Rev. E **88**, 043003 (2013).
[35] E. Yariv and I. Frankel, Electrohydrodynamic rotation of drops at large electric Reynolds numbers, J. Fluid Mech. **788**, R2 (2016).
[36] A. Cebers, E. Lemaire, and L. Lobry, Electrohydrodynamic instabilities and orientation of dielectric ellipsoids in low-conducting fluids, Phys. Rev. E **63**, 016301 (2000).
[37] Y. Dolinsky and T. Elperin, Electrorotation of a leaky dielectric spheroid immersed in a viscous fluid, Phys. Rev. E **80**, 066607 (2009).
[38] Q. Brosseau, G. Hickey, and P. M. Vlahovska, arXiv:1609.04384.
[39] E. Lac and G. M. Homsy, Axisymmetric deformation and stability of a viscous drop in a steady electric field, J. Fluid. Mech. **590**, 239 (2007).
[40] J. A. Lanauze, L. M. Walker, and A. S. Khair, Nonlinear electrohydrodynamics of slightly deformed oblate drops, J. Fluid Mech. **774**, 245 (2015).
[41] D. Das and D. Saintillan, Bull. Am. Phys. Soc. **61**, M16.00001 (2016).
[42] P. B. Binks, Particles as surfactants—Similarities and differences, Curr. Op. Colloid Interface Sci. **7**, 21 (2002).
[43] H. Nganguia, Y. N. Young, P. M. Vlahovska, J. Blawzdziewcz, J. Zhang, and H. Lin, Equilibrium electro-deformation of a surfactant-laden viscous drop, Phys. Fluids **25**, 092106 (2013).
[44] J. W. Ha and S. M. Yang, Effects of surfactant on the deformation and stability of a drop in a viscous fluid in an electric field, J. Colloid Interface Sci. **175**, 369 (1995).
[45] See Supplemental Material at http://link.aps.org/supplemental/10.1103/PhysRevFluids.1.060504 for a movie related to this experiment.

[46] M. Ouriemi and P. M. Vlahovska, Electrohydrodynamic deformation and rotation of a particle-coated drop, Langmuir **31**, 6298 (2015).

[47] C. D. Eggleton, T. M. Tsai, and K. J. Stebe, Tip Streaming from a Drop in the Presence of Surfactants, Phys. Rev. Lett. **87**, 048302 (2001).

[48] S. L. Anna, Droplets and bubbles in microfluidic devices, Annu. Rev. Fluid Mech. **48**, 285 (2016).

[49] Y.-H. Tseng and A. Prosperetti, Local interfacial stability near a zero vorticity point, J. Fluid Mech. **776**, 5 (2015).

[50] Q. Brosseau and P. M. Vlahovska, Bull. Am. Phys. Soc. **61**, M16.00010 (2016).

[51] Z. Rozynek, A. Mikkelsen, P. Dommersnes, and J. O. Fossum, Electroformation of Janus and patchy capsules, Nat. Commun. **5**, 3945 (2014).

[52] Z. Rozynek, R. Castberg, A. Kalicka, P. Jankowski, and P. Garstecki, Electric field manipulation of particles in leaky dielectric liquids, Arch. Mech. **67**, 385 (2015).

[53] Y. Hu, M. Miksis, and P. M. Vlahovska, Bull. Am. Phys. Soc. **61**, L36.00001 (2016).

[54] O. Schnitzer and E. Yariv, The Taylor-Melcher leaky dielectric model as a macroscale electrokinetic description, J. Fluid Mech. **773**, 1 (2015).

[55] M. Z. Bazant, Electrokinetics meets electrohydrodynamics, J. Fluid Mech. **782**, 1 (2015).

[56] P. M. Vlahovska, Voltage-morphology coupling in biomimetic membranes: Dynamics of giant vesicles in applied electric fields, Soft Matter **11**, 7232 (2015).

[57] P. F. Salipante and P. M. Vlahovska, Vesicle deformation in dc electric pulses, Soft Matter **10**, 3386 (2014).

[58] L. C. McConnell, M. J. Miksis, and P. M. Vlahovska, Vesicle dynamics in uniform electric fields: Squaring and breathing, Soft Matter **11**, 4840 (2015).